J. Astrophys. Astr. (2021) 42:4
https://doi.org/10.1007/s12036-020-09650-x

On sensitivity of the stability of equilibrium points with respect to the perturbations

BHAVNEET KAUR[1], SHIPRA CHAUHAN[2,*] and DINESH KUMAR[2]

[1]Department of Mathematics, Lady Shri Ram College for Women, University of Delhi, New Delhi 110 024, India.
[2]Department of Mathematics, University of Delhi, Delhi 110 007, India.
*Corresponding Author. E-mail: chauhanshipra10@gmail.com

MS received 6 May 2020; accepted 6 August 2020

Abstract. The present investigation considers the effect of small perturbations given in the Coriolis and centrifugal forces on the location and stability of the equilibrium points in the Robe's circular restricted three-body problem with non-spherical primary bodies. The felicitous equations of motion of m_3 are obtained by taking into account the shapes of primaries m_1 and m_2, the full buoyancy force of the fluid which is filled inside m_1 of density ρ_1, the forces due to the gravitational attraction of the fluid and m_2. We assume that the massive body m_1 is an oblate spheroid and the m_2 a finite straight segment, and they move under a mutual gravitational attraction described by the Newton's universal law of gravitation. In the present problem, m_3 is moving in the fluid and the rotating reference frame is used, its motion is bound to be affected by the perturbed Coriolis and centrifugal forces. In this attempt these effects along with the effects caused by the oblateness and length parameters A and l respectively, on the location and stability of the equilibrium points are observed. A pair of collinear equilibrium points L_1 and L_2 and infinite number of non-collinear equilibrium points are obtained. The stability of all the equilibrium points depends on the coefficients of their corresponding characteristic polynomials that are obtained with the help of linear variational equations.

Keywords. Oblateness—finite straight segment—Coriolis and centrifugal forces—equilibrium points—stability.

1. Introduction

The general three-body problem is the most celebrated problem in celestial mechanics. Restricted three-body problem is a significant simplification of the general three-body problem, whose importance travels far away from its application to the motion of celestial bodies. In this problem, the motion of an infinitesimal body m_3 is enquired, which moves under the gravitational field of the primary bodies m_1 and m_2. The problem possesses three collinear and two non-collinear equilibrium solutions. The collinear equilibrium points are unstable and the non-collinear ones are stable for the condition that $\mu < \mu_0 = 0.03852\ldots$ (Szebehely 1967a). According to Wintner (1941), since the Coriolis term exists in the equations of motion, the stability of non-collinear equilibrium points can be established.

With respect to various dynamical systems, several researchers have investigated the small perturbing effects in the Coriolis and centrifugal forces. The study of these perturbations, in the context of restricted problem of three bodies, was studied by Szebehely (1967b) who considered the effects of small perturbations only in the Coriolis force and by keeping the centrifugal force constant, to discuss the stability of the equilibrium points. In his study, he concluded that the stability of the collinear equilibrium points remains unaffected by Coriolis effect and thus linearly unstable. For the stability of the non-collinear equilibrium points, he concluded that the Coriolis force is a stabilizing force by obtaining a relation $\mu_c = \mu_0 + \frac{16\epsilon}{3\sqrt{69}}$. Later the extension of his

Published online: 13 February 2021

work was done by Subbarao and Sharma (1975) by considering the shape of bigger primary as an oblate spheroid.

Motivated by the work of Szebehely (1967b) and Subbarao and Sharma (1975), Bhatnagar and Hallan (1978) presented the restricted three-body problem, by examining the position of equilibrium points, in which they allowed the small perturbations ϵ and ϵ' given to the Coriolis and centrifugal forces respectively. They pointed out that for the non-collinear equilibrium points, the range of stability changes the $\epsilon\epsilon'$-plane. However, the instability of the collinear equilibrium points remains unaffected by the perturbations. Following the procedure of Deprit and Deprit-Bartholme (1967), Bhatnagar and Hallan (1983) carried out a study to discuss the non-linear stability of the equilibrium points obtained in Bhatnagar and Hallan (1978).

Since then the perturbed restricted three-body problem continues to attract many researchers, and numerous studies regarding equilibrium points in restricted three-body problem has been reported. Some of the variants of this problem has been studied by AbdulRaheem & Singh (2006), Kushvah (2008), Abouelmagd *et al.* (2013), Singh and Bello (2014), and Singh & Haruna (2014).

Robe (1977) pioneered the study related to the motion of an infinitesimal body with respect to the primary bodies. In his problem, the infinitesimal body m_3 assumes the shape of a rigid spherical shell with density ρ_3, is embedded in the more massive primary m_1 which itself is filled with an homogeneous incompressible fluid of density ρ_1, and the less massive primary m_2 lies outside m_1. He assumed that m_3 is influenced by the gravitational attractions of m_1 and m_2 and the buoyancy force of the fluid. He obtained an equilibrium point that lies at the centre of m_1, and found the regions of stability under certain conditions.

The Robe's problem assumes that the infinitesimal body moves under the influence of the mutual gravitational attraction of the primary bodies and the buoyancy force of the fluid. But in general, the Coriolis and centrifugal forces are effective and the small perturbations also affect the motion of infinitesimal body, where these small perturbations are the consequence of the lack of sphericity of the primary bodies, the atmospheric drag, and viscosity of the fluid on the motion of the other celestial bodies. Many researchers have worked with these small perturbations in the Coriolis and centrifugal forces, and oblateness of the primaries. They examined the effect of these perturbations on the location and linear stability of the equilibrium points.

Shrivastava and Garain (1991) studied the abovementioned perturbing effects on the position of equilibrium points in the Robe's restricted three-body problem for the case when $\rho_1 = \rho_3$. The effect of such perturbations was noticed on the location of equilibrium point $\left(-\mu + \frac{\epsilon'\mu}{1+2\mu}, 0, 0\right)$. The continuation to their work was carried out by Si-hui and Ben-kui (2005) with the assumption that $\rho_1 \leq \rho_3$. They obtained the condition for the existence of equilibrium points in the perturbed Robe's problem and discussed the linear stability of the obtained equilibrium points.

Plastino and Plastino (1995) revisited the Robe's problem by considering the hydrostatic equilibrium figure of m_1 as a Roche's ellipsoid. Additionally, they studied the motion of infinitesimal body by taking those components of the pressure field that are originating due to the gravitational field of the fluid, attraction of m_2 and the centrifugal force. Later, the problems of Robe (1977) and Plastino and Plastino (1995) were studied by Giordano *et al.* (1997) with regard to the effect of a linear drag force.

Hallan and Rana (2001b) studied the location and stability of the equilibrium point obtained by Robe (1977) under the small perturbations ϵ and ϵ' to the Coriolis and centrifugal forces respectively for the case when $\rho_1 = \rho_3$. On taking the perturbations, they obtained only one equilibrium point $\left(-\mu + \frac{\mu\epsilon'}{1+2\mu}, 0, 0\right)$, which is towards the right or left of the centre of m_1 depending on the sign of ϵ'. They also drew some conclusions regarding the stability of the equilibrium point. Moreover, Hallan and Mangang (2008) proposed a study to describe the effect of these perturbations on the nonlinear stability of the equilibrium point.

A huge number of research work is devoted to examining the location and stability of the equilibrium points in the Robe's problem with variations in the shape of the primaries (Hallan & Mangang 2007; Singh & Sandah 2012; Singh & Mohammed 2012, 2013; Ansari *et al.* 2019). The extension of Robe's problem to the Robe's problem of 2+2 bodies was done by Kaur & Aggarwal (2012, 2013a, b), and Aggarwal & Kaur (2014).

Recently, Kumar *et al.* (2019) modified the problem of Robe by taking the shape of m_2 as a finite straight segment. Their results are in accordance with Hallan and Rana (2001a) in the absence of the finite straight segment. They made an effort to study the changes in the position and stability of the equilibrium points due to the effect of the length parameter. On taking the small perturbations in the Coriolis and centrifugal forces in their work, Kaur *et al.* (2020) discussed how these small perturbations affect the location and stability of the equilibrium points.

Taking into consideration all the efforts put up by the afore-mentioned authors in their works, we were able to obtain a vision for our work which has been been subsequently explained in this paper. The structure of the problem and the equations of motion are defined in Section 2. Equilibrium points are obtained in Section 3 by using the necessary and sufficient conditions. This section also includes the numerical investigation of the equilibrium points for various parameters involved in the problem, through which the effect of small perturbations is noticed. The linear stability analysis of all the equilibrium points that are obtained for the present problem is presented in Section 4. Application of the presented mathematical model is presented in Section 5. Section 6 concludes the paper.

2. Mathematical formulation of the problem

Consider the primary bodies of masses m_1 and m_2 ($m_1 >> m_2$). The massive primary body m_1 assumes the shape of oblate spheroid as taken by Hallan and Mangang (2007) with an homogeneous incompressible fluid of density ρ_1 filled inside it. The less massive body m_2 is taken as the finite straight segment of length $2l$ as in Kumar *et al.* (2019), that describes a circular orbit around m_1. We consider a uniformly rotating coordinate system $Oxyz$ with origin at the centre of the mass of m_1, Ox points towards m_2 and Oxy being the orbital plane of m_2.

Using dimensionless variables, the governing equations of motion of m_3 in this coordinate system as in Hallan and Mangang (2007) under the perturbing effects in the rotating coordinate system are

$$\ddot{x} - 2\alpha n\dot{y} = U_x, \tag{1a}$$

$$\ddot{y} + 2\alpha n\dot{x} = U_y, \tag{1b}$$

$$\ddot{z} = U_z, \tag{1c}$$

where

$$\begin{aligned}
U(x,y,z) = \rho\Big[\pi\rho_1(I - A_1x^2 - A_1y^2 - A_2z^2) \\
+\frac{1}{2}n^2\beta((x-\mu)^2 + y^2) \\
+\frac{\mu}{2l}\log\left(\frac{r_1 + r_2 + 2l}{r_1 + r_2 - 2l}\right)\Big],
\end{aligned}$$

$$\begin{aligned}
&\alpha = 1 + \epsilon_1, \ |\epsilon_1| < < 1, \\
&\beta = 1 + \epsilon_2, \ |\epsilon_2| < < 1, \\
&n^2 = 1 + l^2 + \frac{3}{2}A, \ 0 < l < < 1, \\
&A = \frac{a_1^2 - a_2^2}{5R^2}, 0 < A < < 1, \\
&\mu = \frac{m_2}{m_1 + m_2}, \quad 0 < \mu < 1, \\
&\rho = 1 - \frac{\rho_1}{\rho_3}, \\
&r_1^2 = (x - 1 + l)^2 + y^2 + z^2, \\
&r_2^2 = (x - 1 - l)^2 + y^2 + z^2.
\end{aligned}$$

Here U is the potential that explains the combined action of the three forces acting on m_3, the gravitational force exerted by the fluid and m_2, and the buoyancy force of the fluid. The suffixes x, y and z denote the partial derivatives of U with respect to x, y and z respectively, and dot signifies the differentiation with respect to time in dimensionless variables. The parameters ϵ_1 and ϵ_2 denote the small perturbations given to the Coriolis and centrifugal forces respectively. The polar moment of inertia of the oblate primary is given by

$$I = 2a_1^2A_1 + a_2^2A_2,$$

where

$$\begin{aligned}
A_1 = a_1^2a_2\int_0^\infty \frac{\mathrm{d}u}{\Delta(a_1^2 + u)}, \\
A_2 = a_1^2a_2\int_0^\infty \frac{\mathrm{d}u}{\Delta(a_2^2 + u)},
\end{aligned}$$

and $\Delta^2 = (a_1^2 + u)^2(a_2^2 + u)$

with a_1 and a_2 its dimensionless equatorial and polar radii, A is the oblateness coefficient and R is the distance between the primaries. If the effect of small perturbations in the Coriolis and centrifugal forces is not considered and the shape of the smaller primary is assumed to be a point mass instead of finite straight segment, the equations of motion (1a)–(1c) completely agree with Hallan and Mangang (2007).

3. Equilibrium points

The existence of equilibrium points depends on the necessary as well as sufficient conditions are $\dot{x} = \dot{y} = \dot{z} = \ddot{x} = \ddot{y} = \ddot{z} = 0$.

The simultaneous solution of the following equations is needed to obtain the coordinates (x, y, z) of equilibrium points

$$U_x = 0, \quad U_y = 0 \quad \text{and} \quad U_z = 0.$$

Therefore, the equilibrium points are obtained by solving the following equations simultaneously:

$$\rho\left[n^2(x-\mu)\beta - 2\pi\rho_1 A_1 x - \frac{2\mu}{[(r_1+r_2)^2-4l^2]} \times \left(\frac{x-1+l}{r_1} + \frac{x-1-l}{r_2}\right)\right] = 0, \tag{2a}$$

$$\rho\left[n^2\beta - 2\pi\rho_1 A_1 - \frac{2\mu}{[(r_1+r_2)^2-4l^2]} \times \left(\frac{1}{r_1} + \frac{1}{r_2}\right)\right] y = 0, \tag{2b}$$

$$\rho\left[2\pi\rho_1 A_2 + \frac{2\mu}{[(r_1+r_2)^2-4l^2]}\left(\frac{1}{r_1} + \frac{1}{r_2}\right)\right] z = 0. \tag{2c}$$

The above equations are all independent of α, therefore the positions of the equilibrium points are not affected by the small perturbations in the Coriolis force. It is to note that the density parameter $\rho \neq 0$. If so, $\rho_1 = \rho_3$ which violates our assumption of unequal densities.

In Equation (2c),

$$2\pi\rho_1 A_2 + \frac{2\mu}{[(r_1+r_2)^2-4l^2]}\left(\frac{1}{r_1} + \frac{1}{r_2}\right) \neq 0,$$

for the defined values of the parameters involved, which gives $z = 0$. Therefore, the motion of m_3 is possible only in the xy-plane, that is, in the plane of motion of the primary bodies. Our study is then limited to the coplanar equilibrium points, the points located in the xy-plane with $z = 0$.

3.1 *Collinear equilibrium points*

The collinear equilibrium points are obtained from Equations (2a) and (2b) by taking $y = 0$. These points are the solution of the following equation:

$$n^2(x-\mu)\beta - 2\pi\rho_1 A_1 x - \frac{2\mu}{[(r_1+r_2)^2-4l^2]} \times \left(\frac{x-1+l}{r_1} + \frac{x-1-l}{r_2}\right) = 0,$$

where $r_1 = |x-1+l|$ and $r_2 = |x-1-l|$. The above equation can be recast into the following form:

$$\left(1 + l^2 + \frac{3}{2}A\right)(x-\mu)\beta - 2\pi\rho_1 A_1 x - \frac{\mu}{[l^2-(x-1)^2]} = 0. \tag{3}$$

When $A = 0$, $l = 0$ and $\epsilon_2 = 0$, the two solutions of Eq. (3) are $x_1 = 0$ and

$$x_2 = 1 + \frac{\mu + \sqrt{\mu^2 + 8\pi\rho_1 A_1 \mu - 4\mu}}{2(1-2\pi\rho_1 A_1)},$$

(Hallan & Mangang 2007)

provided $1 - 2\pi\rho_1 A_1 + \frac{3}{4}\mu < 0$ and $|x_2| < a_1$.

Next, we aim to find the roots of Eq. (3) when $A \neq 0$, $l \neq 0$ and $\epsilon_2 \neq 0$. Let the roots of Eq. (3) for this case be

$$x^{(1)} = x_1 + p_1 \quad \text{and} \quad x^{(2)} = x_2 + p_2 \text{ with } |p_i| << 1, \quad i = 1, 2,$$

where the expressions for p_1 and p_2 are calculated by putting the above values in Eq. (3) and by retaining only the first order terms of p_1, p_2, A and up to second order terms of l,

$$p_1 \cong \frac{\mu}{2}\left(\frac{2\epsilon_2 + 3A}{1 + 2\mu - 2\pi\rho_1 A_1}\right)$$

and

$$p_2 = \frac{-\mu l^2(1-x_2)^{-3} + (x_2-\mu)(x_2-1)(l^2 + \frac{3A}{2} + \epsilon_2)}{2\mu + (1-2\pi\rho_1 A_1)(1-3x_2)}.$$

Therefore, when A, l and ϵ_2 are present, $L_1(x^{(1)}, 0, 0)$ is always an equilibrium point and $L_2(x^{(2)}, 0, 0)$ is another equilibrium point which exist only if $1 - 2\pi\rho_1 A_1 < -\frac{3\mu}{4}$ and $|x^{(2)}| < a_1$. When $\epsilon_1 = \epsilon_2 = l = 0$, the collinear equilibrium points L_1 and L_2 coincide with Hallan and Mangang (2007).

For the fixed values of $\rho_1 = 0.649$, $A_1 = 0.3$, $\mu = 0.1$ and $l = 0.0001$, the effect of small perturbation in the centrifugal force and oblateness on the positions of L_1 and L_2 are numerically calculated in Table 1. It is observed that, with the increasing values of ϵ_2, the equilibrium point L_1 drifts away from the centre of the bigger primary in the left direction, however L_2 moves towards the smaller primary.

The effect of small perturbation in the centrifugal force with respect to mass and length parameters is given in Tables 2 and 3 respectively. It can be seen that, as the parameter ϵ_2 is increased, the equilibrium point L_1 drifts away from the centre of the bigger primary in the left direction and L_2 moves towards the centre of the bigger primary.

From Fig. 1, it is evident how the small perturbation in the centrifugal force ϵ_2 affects the positions of the collinear equilibrium points L_1 and L_2. We have fixed the parameters $\rho_1 = 0.649$, $A_1 = 0.3$, $\mu = 0.1$, $l = 0.0001$ and $A = 0.01$. It is perceived that as we give an increment in ϵ_2 from 0.02 to 0.06 with step size 0.01, L_1 drifts away from the centre of the bigger primary m_1 in the negative direction of x-axis and L_2 eventually moves towards the centre of the smaller primary m_2 along the x-axis.

3.2 *Non-collinear equilibrium points*

The locations of non-collinear equilibrium points are evaluated by taking $x \neq 0$ and $y \neq 0$ in Equations (2a) and (2b). These points are obtained by solving the following equations simultaneously:

$$n^2(x-\mu)\beta - \frac{2\mu}{[(r_1+r_2)^2 - 4l^2]} \times \left(\frac{x-1+l}{r_1} + \frac{x-1-l}{r_2}\right) - 2\pi\rho_1 A_1 x = 0, \tag{4a}$$

$$n^2\beta - \frac{2\mu}{[(r_1+r_2)^2 - 4l^2]}\left(\frac{1}{r_1} + \frac{1}{r_2}\right) - 2\pi\rho_1 A_1 = 0. \tag{4b}$$

On solving the above equations, we have

$$(1-x)^2 + y^2 = \left[1 - \left(A + \frac{2}{3}l^2\right)\right]\left(1 - \frac{2}{3}\epsilon_2\right). \tag{5}$$

The points on the above circle are the non-collinear equilibrium points provided

$$2\pi\rho_1 A_1 = (1-\mu)\left(1 + \frac{3}{2}A + l^2\right)(1+\epsilon_2).$$

These points are affected by the small perturbation in the centrifugal force, oblateness and length parameters.

4. Stability analysis

A real system is subject to disturbances, therefore, it is of considerable practical interest to inquire as to its response to these disturbances. The stability analysis describes its behaviour to the disturbances. The motion that remains in the small neighborhood of the equilibrium point after it is disturbed is termed as stable.

The stability analysis of equilibrium points formally presents the problem of studying the behaviour of the infinitesimal mass m_3, where the equilibrium point $L(x_0, y_0, z_0)$ is displaced as

$$\left.\begin{aligned} x &= x_0 + \xi, \\ y &= y_0 + \eta, \\ z &= z_0 + \zeta, \end{aligned}\right\} \xi, \eta, \zeta \ll 1,$$

where ξ, η and ζ are the small perturbations in the x, y and z directions respectively. Then the linearized variational equations corresponding to the equations of motion are

$$\ddot{\xi} - 2n\alpha\dot{\eta} = U^L_{xx}\xi + U^L_{xy}\eta + U^L_{xz}\zeta, \tag{6a}$$

$$\ddot{\eta} + 2n\alpha\dot{\xi} = U^L_{yx}\xi + U^L_{yy}\eta + U^L_{yz}\zeta, \tag{6b}$$

$$\ddot{\zeta} = U^L_{zx}\xi + U^L_{zy}\eta + U^L_{zz}\zeta, \tag{6c}$$

where the subscripts x, y and z denote the second-order partial derivatives of $U(x, y, z)$ and superscript L indicates that the derivatives are to be determined at one of the equilibrium points.

We are only interested in the motion in the immediate vicinity of the equilibrium points, and therefore, it is legitimate to neglect the higher-order terms since these will always be small quantities, provided we only consider a small initial displacement from the equilibrium point (x_0, y_0, z_0).

4.1 *Stability of the collinear equilibrium point L_1*

At the collinear equilibrium point L_1, we have

$$U^{L_1}_{xx} = \frac{\rho\mu}{2}\left(\frac{2\epsilon_2 + 3A}{p_1}\right),$$
$$U^{L_1}_{xy} = U^{L_1}_{xz} = U^{L_1}_{yz} = 0,$$
$$U^{L_1}_{yy} = \frac{\rho\mu}{2}\left[\left(\frac{2\epsilon_2 + 3A}{p_1}\right) - 6\right],$$
$$U^{L_1}_{zz} = -\rho\left[\mu + 2\pi\rho_1 A_2 + 2\mu l^2 + 3\mu p_1\right].$$

On substituting the above second-order derivatives in the variational equations (6a)–(6c), we obtain

Table 1. The abscissae of the collinear equilibrium points L_1 and L_2 when $\rho_1 = 0.649$, $A_1 = 0.3$, $\mu = 0.1$, and $l = 0.0001$.

$A \rightarrow$	10^{-6}		0.004		0.01		0.02		0.04	
$\epsilon_2 \downarrow$	L_1	L_2	L_1	L_2	L_1	L_2	L_1	L_2	L_1	L_2
0.02	−0.0799888	0.0821950	−0.1051200	0.0839460	−0.1447910	0.0859648	−0.2179430	0.0883457	−0.4035260	0.0912430
0.03	−0.1215720	0.0848728	−0.1487410	0.0861299	−0.1921860	0.0876459	−0.2735600	0.0895221	−0.4855410	0.0919292
0.04	−0.1662310	0.0868009	−0.1960570	0.0877590	−0.2442120	0.0889496	−0.3356570	0.0904749	−0.5806000	0.0925135
0.05	−0.2148850	0.0882687	−0.2479960	0.0890289	−0.3019110	0.0899944	−0.4056940	0.0912640	−0.6922510	0.0930174
0.06	−0.2684690	0.0894295	−0.3055850	0.0900506	−0.3665290	0.0908526	−0.4855410	0.0919292	−0.8257970	0.0934566

Table 2. The abscissae of the collinear equilibrium points L_1 and L_2 when $\rho_1 = 0.649$, $A_1 = 0.3$, $A = 10^{-6}$, and $l = 0.0001$.

$\mu \rightarrow$	0.01		0.05		0.1		0.13		0.15	
$\epsilon_2 \downarrow$	L_1	L_2	L_1	L_2	L_1	L_2	L_1	L_2	L_1	L_2
0.02	−0.0010908	0.7524650	−0.0017303	0.7455380	−0.0024480	0.7380230	−0.0032589	0.7298340	−0.0048248	0.7208640
0.03	−0.0095474	0.3713020	−0.0156848	0.3547140	−0.0230711	0.3372250	−0.0320737	0.3188580	−0.0431918	0.2996850
0.04	−0.0799888	0.0821950	−0.1215720	0.0848728	−0.1662310	0.0868009	−0.2148850	0.0882687	−0.2684690	0.0894295
0.05	−0.2285090	0.0363378	−0.2859920	0.0455719	−0.3461470	0.0526619	−0.4105450	0.0583792	−0.4805980	0.0631393
0.06	−0.3441510	0.0274080	−0.4074910	0.0363371	−0.4746730	0.0436351	−0.5470960	0.0497845	−0.6261910	0.0550792

Table 3. The abscissae of the collinear equilibrium points L_1 and L_2 when $\rho_1 = 0.649$, $A = 10^{-6}$, $\mu = 0.1$, and $A_1 = 0.3$.

$l \rightarrow$	0.0001		0.005		0.01		0.05		0.1	
$\epsilon_2 \downarrow$	L_1	L_2	L_1	L_2	L_1	L_2	L_1	L_2	L_1	L_2
0.02	−0.0799888	0.0821950	−0.1215720	0.0848728	−0.1662310	0.0868009	−0.2148850	0.0882687	−0.2684690	0.0894295
0.03	−0.0800505	0.0821396	−0.1216520	0.0848259	−0.1663280	0.0867599	−0.2150000	0.0882322	−0.2686040	0.0893964
0.04	−0.0802362	0.0819735	−0.1218920	0.0846853	−0.1666200	0.0866370	−0.2153460	0.0881226	−0.2690080	0.0892974
0.05	−0.0864176	0.0768077	−0.1298180	0.0803096	−0.1762110	0.0828097	−0.2266660	0.0847063	−0.282220	0.0862043
0.06	−0.1088470	0.0625698	−0.1575630	0.0681588	−0.2091920	0.0720965	−0.2652360	0.0750732	−0.3270520	0.0774251

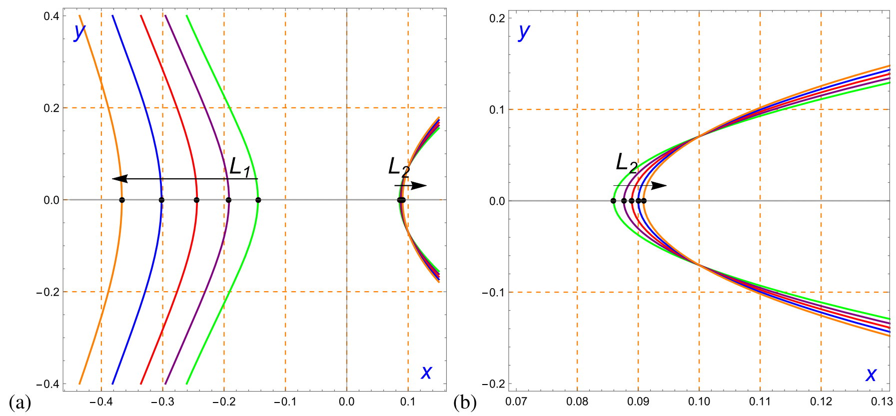

Figure 1. **(a)** The color curves represent the function $U_x(x, y)$. The positions of the collinear equilibrium points (black dots) for the fixed values of $\rho_1 = 0.649$, $A_1 = 0.3$, $\mu = 0.1$, $l = 0.0001$, $A = 0.01$ and increasing values of the perturbation in the centrifugal force $\epsilon_2 = 0.02$ (green), 0.03 (purple), 0.04 (red), 0.05 (blue), 0.06 (orange). The arrows with black color point out the movement of the collinear equilibrium points. **(b)** The zoomed area near L_2.

$$\ddot{\xi} - 2n\alpha\dot{\eta} = U^{L_1}_{xx}\xi, \tag{7a}$$

$$\ddot{\eta} + 2n\alpha\dot{\xi} = U^{L_1}_{yy}\eta, \tag{7b}$$

$$\ddot{\zeta} = U^{L_1}_{zz}\zeta. \tag{7c}$$

Note that for all the values of the parameters involved, $U^{L_1}_{zz} < 0$, therefore the motion of the infinitesimal body parallel to the z-axis is always stable. Thus, it suffices to check the stability of motion of the infinitesimal body in the xy-plane only.

Let $(B_1 e^{\lambda t}, B_2 e^{\lambda t})$ be the trial solution of the system of Equations (7a) and (7b). On substituting these solutions in Equations (7a) and (7b), we obtain

$$(\lambda^2 - U^{L_1}_{xx})B_1 + (-2n\alpha\lambda)B_2 = 0,$$
$$(2n\alpha\lambda)B_1 + (\lambda^2 - U^{L_1}_{yy})B_2 = 0.$$

The above equations hold a non-trivial solution if

$$\begin{vmatrix} \lambda^2 - U^{L_1}_{xx} & -2n\alpha\lambda \\ 2n\alpha\lambda & \lambda^2 - U^{L_1}_{yy} \end{vmatrix} = 0.$$

Then the corresponding characteristic equation is

$$\lambda^4 + w_1\lambda^2 + w_2 = 0, \tag{8}$$

where

$$w_1 = (4n^2\alpha^2 - U^{L_1}_{xx} - U^{L_1}_{yy}) \quad \text{and} \quad w_2 = U^{L_1}_{xx}U^{L_1}_{yy}.$$

An equilibrium point is said to be stable if all the roots of the characteristic equation are either negative real numbers, or distinct and purely imaginary numbers, or complex numbers having negative real parts. Therefore, the stability of the collinear equilibrium point L_1 depends on the coefficients w_1 and w_2 of the characteristic Eq. (8). On taking $\Lambda = \lambda^2$, we have

$$\Lambda_{1,2} = \frac{-w_1 \pm \sqrt{\gamma}}{2}, \quad \text{where } \gamma = w_1^2 - 4w_2.$$

Under the influence of the perturbations, the equilibrium point L_1 will be stable if Λ_1 and Λ_2 are real and negative. That is, the conditions of stability yield $\Lambda_1 + \Lambda_2 < 0$ and $\Lambda_1\Lambda_2 > 0$, that consequently leads to the following three conditions:

$$w_1 > 0, \quad w_2 > 0, \quad \text{and} \quad w_1^2 - 4w_2 > 0. \tag{9}$$

In Fig. 2, the light blue color represents the region

$$R_1 = \{(\epsilon_1, \epsilon_2) : w_1 > 0,\ w_2 > 0 \quad \text{and} \quad w_1^2 - 4w_2 > 0\},$$

with $-1 < \epsilon_1, \epsilon_2 < 1$, for the fixed values of the parameters $\rho_1 = 0.649$, $A = 0.01$, $\mu = 0.1$, $A_1 = 0.3$, $l = 0.0001$ and $\rho = 0.2$. In this pictorial representation, it can be seen that the collinear equilibrium point L_1 is stable for all the combinations of ϵ_1 and ϵ_2.

In Table 4, the conditions of stability (9) are evaluated at L_1 for the fixed values of some parameters involved in the problem. For the numerical investigation, we take $\rho_1 = 0.649$, $\mu = 0.1$, $A_1 = 0.3$, $l = 0.0001$, $A = 0.01$, $\rho = 0.2$. It is observed that for the varying ϵ_1 and ϵ_2 in the range $(-0.9, 0.9)$ with step size 0.2, all the stability conditions are satisfied. Thus, L_1 is stable for these fixed set of parameters.

4.2 *Stability of the collinear equilibrium point L_2*

The variational equations (6a)–(6c) are obtained as follows:

$$\ddot{\xi} - 2n\alpha\dot{\eta} = U_{xx}^{L_2}\xi, \tag{10a}$$

$$\ddot{\eta} + 2n\alpha\dot{\xi} = U_{yy}^{L_2}\eta, \tag{10b}$$

$$\ddot{\zeta} = U_{zz}^{L_2}\zeta, \tag{10c}$$

where

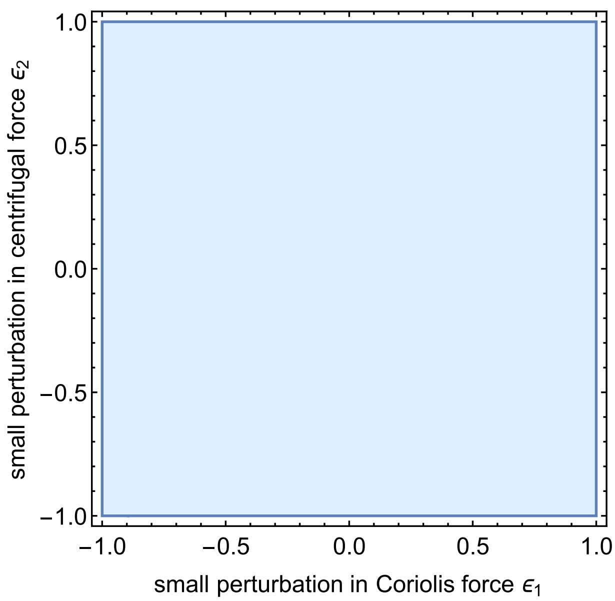

Figure 2. The light blue region represents the stability conditions (9) in $\epsilon_1\epsilon_2$-plane for the fixed values of the parameters $\rho_1 = 0.649$, $A = 0.01$, $\mu = 0.1$, $A_1 = 0.3$, $l = 0.0001$ and $\rho = 0.2$.

$$U_{xx}^{L_2} = \rho\left[1 + \epsilon_2 - 2\pi\rho_1 A_1 + \frac{2\mu}{(-1 + x^{(2)})^3} + \frac{3A}{2}(1+\epsilon_2) + \left(1 + \epsilon_2 + \frac{4\mu}{(-1 + x^{(2)})^5}\right)l^2\right],$$

$$U_{yy}^{L_2} = \rho\left[1 + \epsilon_2 - 2\pi\rho_1 A_1 - \frac{\mu}{(-1 + x^{(2)})^3} + \frac{3A}{2}(1+\epsilon_2) + \left(1 + \epsilon_2 - \frac{2\mu}{(-1 + x^{(2)})^5}\right)l^2\right],$$

$$U_{zz}^{L_2} = -2\rho\left[\pi\rho_1 A_2 + \frac{\mu}{2(1 - x^{(2)})^3} + \frac{\mu l^2}{(-1 + x^{(2)})^5}\right].$$

As for the stability of L_1 in Section 4.1, the characteristic equation corresponding to the variational equations (10a) and (10b) is given by

$$\lambda^4 + w_3\lambda^2 + w_4 = 0,$$

with

$$w_3 = (4n^2\alpha^2 - U_{xx}^{L_2} - U_{yy}^{L_2}) \quad \text{and} \quad w_4 = U_{xx}^{L_2} U_{yy}^{L_2}.$$

If λ_1^2 and λ_2^2 are the roots of the characteristic equation, then $\lambda_1^2 + \lambda_2^2 = -w_3$ and $\lambda_1^2\lambda_2^2 = w_4$. Therefore for the collinear equilibrium point L_2 to be stable, we must have

$$w_3 > 0, \quad w_4 > 0, \quad \text{and} \quad w_3^2 - 4w_4 > 0. \tag{11}$$

In Fig. 3, for the stability of L_2, the permissible values of ϵ_1 and ϵ_2 are obtained by plotting the stability conditions that are given by Equations (11), for the fixed values of the parameters $\rho_1 = 0.649$, $\mu = 0.1$, $A_1 = 0.3$, $l = 0.1$, $\rho = 0.2$ and different values of the oblateness parameter $A = 10^{-6}, 0.1, 0.15, 0.2$. The

Table 4. The stability of the collinear equilibrium point L_1 for the fixed values of the parameters $\rho_1 = 0.649$, $\mu = 0.1$, $A_1 = 0.3$, $l = 0.0001$, $A = 0.01$ and $\rho = 0.2$.

$\epsilon_2 \rightarrow$ $\epsilon_1 \downarrow$	−0.9	−0.7	−0.5	−0.3	−0.1	0.1	0.3	0.5	0.7	0.9
−0.9	stable	stable	stable	stable	stable	stable	stable	stable	stable	stable
−0.7	stable	stable	stable	stable	stable	stable	stable	stable	stable	stable
−0.5	stable	stable	stable	stable	stable	stable	stable	stable	stable	stable
−0.3	stable	stable	stable	stable	stable	stable	stable	stable	stable	stable
−0.1	stable	stable	stable	stable	stable	stable	stable	stable	stable	stable
0.1	stable	stable	stable	stable	stable	stable	stable	stable	stable	stable
0.3	stable	stable	stable	stable	stable	stable	stable	stable	stable	stable
0.5	stable	stable	stable	stable	stable	stable	stable	stable	stable	stable
0.7	stable	stable	stable	stable	stable	stable	stable	stable	stable	stable
0.9	stable	stable	stable	stable	stable	stable	stable	stable	stable	stable

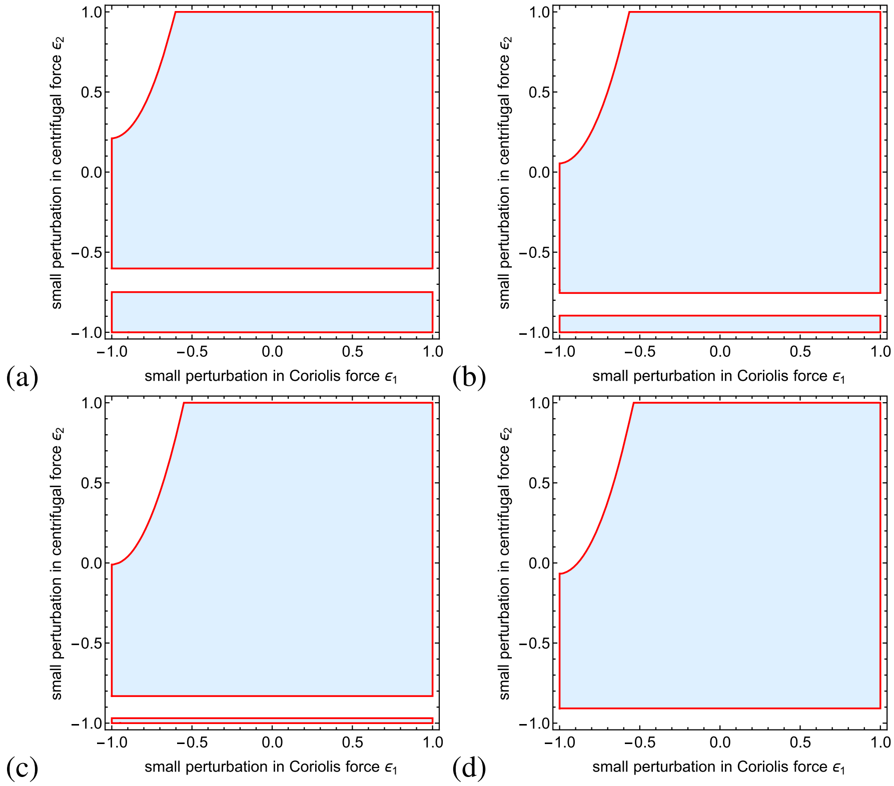

Figure 3. The light blue region represents the stability conditions (11) for the fixed values of the parameters $\rho_1 = 0.649$, $\mu = 0.1$, $A_1 = 0.3$, $l = 0.1$ and $\rho = 0.2$. **(a)** $A = 10^{-6}$, **(b)** $A = 0.1$, **(c)** $A = 0.15$, **(d)** $A = 0.2$.

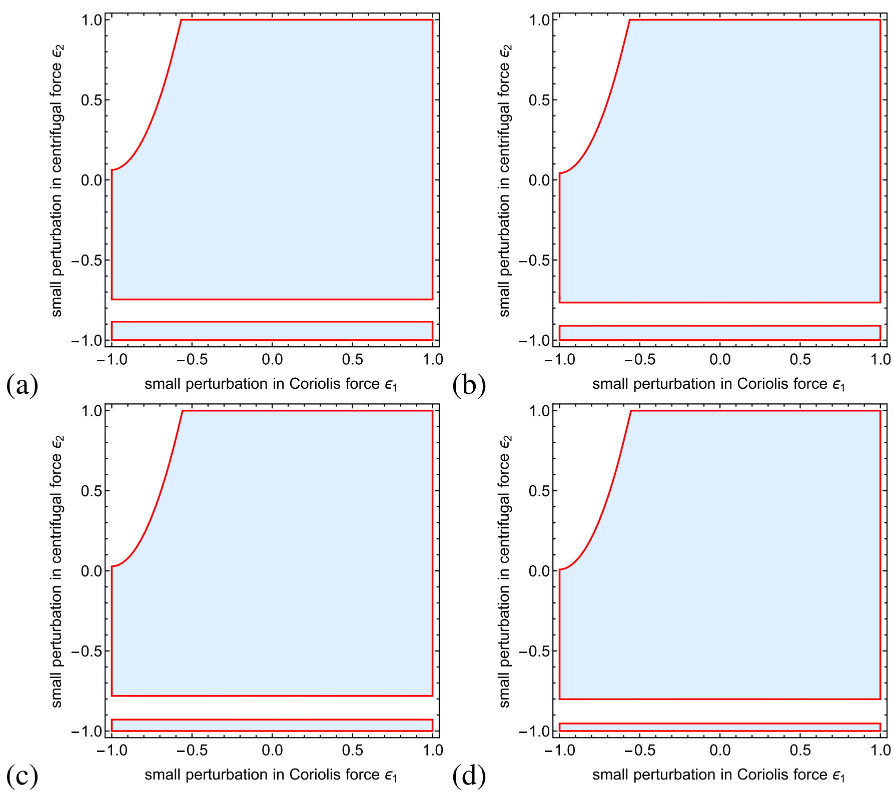

Figure 4. The light blue region represents the stability conditions (11) for the fixed values of the parameters $\rho_1 = 0.649$, $\mu = 0.1$, $A_1 = 0.3$, $A = 0.1$ and $\rho = 0.2$. **(a)** $l = 0.0001$, **(b)** $l = 0.15$, **(c)** $l = 0.2$, **(d)** $l = 0.25$.

equilibrium point L_2 is stable for all the values of ϵ_1 and ϵ_2 lying in the region

$$R_2 = \{(\epsilon_1, \epsilon_2) : w_3 > 0,\ w_4 > 0 \text{ and } w_3^2 - 4w_4 > 0\},$$

with $-1 < \epsilon_1, \epsilon_2 < 1$, that is shown by the light blue color. However, it is unstable for the values of ϵ_1 and ϵ_2 outside the region R_2.

Further, from Figures 3(a), (b), (c) and (d), it has been observed that for the above fixed values of the parameters, the region R_2 changes for the different values of the oblateness parameter $A = 10^{-6}, 0.1, 0.15$ and 0.2. Similar changes are noticed in Figures 4(a), (b), (c) and (d) for the fixed values of $\rho_1 = 0.649$, $\mu = 0.1$, $A_1 = 0.3$, $A = 0.1$, $\rho = 0.2$ and different values of the length parameter $l = 0.0001, 0.15, 0.2$ and 0.25.

In Table 5, the stability of L_2 is numerically evaluated for the fixed values of $\rho_1 = 0.649$, $\mu = 0.1$, $A_1 = 0.3$, $l = 0.1$, $A = 10^{-6}$ and $\rho = 0.2$. For the step size 0.2 in the range $(-0.9, 0.9)$ of ϵ_1 and ϵ_2, it can be seen that L_2 is unstable for some set of values (ϵ_1, ϵ_2).

4.3 *Stability of the non-collinear equilibrium points*

The general coordinates of any point on the circle

$$(1-x)^2 + y^2 = r^2$$

for a parameter θ is denoted by $(1 + r\cos\theta, r\sin\theta, 0)$, where

$$r^2 = \left[1 - \left(A + \frac{2}{3}l^2\right)\right]\left(1 - \frac{2}{3}\epsilon_2\right).$$

The second-order partial derivatives of $U(x, y, z)$ at this circular point are

$$U_{xx}^c = \rho\mu\left[3\left(1 + \epsilon_2 + \frac{3}{2}A\right)\cos^2\theta + \frac{1}{16}(33 + 44\cos 2\theta + 35\cos 4\theta)l^2\right],$$

$$U_{yy}^c = \rho\mu\left[3\left(1 + \epsilon_2 + \frac{3}{2}A\right)\sin^2\theta + \frac{1}{16}(27 - 24\cos 2\theta - 35\cos 4\theta)l^2\right],$$

$$U_{zz}^c = -\rho\left[2\pi\rho_1 A_2 + \left(1 + \epsilon_2 + \frac{3}{2}A\right)\mu + \frac{1}{4}\mu(7 + 5\cos 2\theta)l^2\right],$$

$$U_{xy}^c = \rho\mu\left[3\left(1 + \epsilon_2 + \frac{3}{2}A\right)\sin\theta\cos\theta + \frac{1}{8}\sin\theta(69\cos\theta + 35\cos 3\theta)l^2\right],$$

$$U_{yz}^c = 0 \text{ and } U_{xz}^c = 0.$$

The variational equations (6a)–(6c) are further reduced as follows:

$$\ddot{\xi} - 2n\alpha\dot{\eta} = U_{xx}^c\xi + U_{xy}^c\eta, \tag{12a}$$

$$\ddot{\eta} + 2n\alpha\dot{\xi} = U_{xy}^c\xi + U_{yy}^c\eta, \tag{12b}$$

$$\ddot{\zeta} = U_{zz}^c\zeta, \tag{12c}$$

The characteristic equation corresponding to the variational equations (12a) and (12b) is given by

Table 5. The stability of the collinear equilibrium point L_2 for the fixed values of the parameters $\rho_1 = 0.649$, $\mu = 0.1$, $A_1 = 0.3$, $l = 0.1$, $A = 10^{-6}$ and $\rho = 0.2$.

$\epsilon_2 \rightarrow \epsilon_1 \downarrow$	−0.9	−0.7	−0.5	−0.3	−0.1	0.1	0.3	0.5	0.7	0.9
−0.9	stable	unstable	stable	stable	stable	stable	unstable	unstable	unstable	unstable
−0.7	stable	unstable	stable	stable	stable	stable	stable	stable	unstable	unstable
−0.5	stable	unstable	stable	stable	stable	stable	stable	stable	stable	stable
−0.3	stable	unstable	stable	stable	stable	stable	stable	stable	stable	stable
−0.1	stable	unstable	stable	stable	stable	stable	stable	stable	stable	stable
0.1	stable	unstable	stable	stable	stable	stable	stable	stable	stable	stable
0.3	stable	unstable	stable	stable	stable	stable	stable	stable	stable	stable
0.5	stable	unstable	stable	stable	stable	stable	stable	stable	stable	stable
0.7	stable	unstable	stable	stable	stable	stable	stable	stable	stable	stable
0.9	stable	unstable	stable	stable	stable	stable	stable	stable	stable	stable

$\lambda^4 + w_5\lambda^2 + w_6 = 0,$

where $w_5 = 4n^2\alpha^2 - U^c_{xx} - U^c_{xy}$ and $w_6 = U^c_{xx}U^c_{yy} - (U^c_{xy})^2$. The non-collinear equilibrium points will be stable if $w_5 > 0$, $w_6 > 0$ and $w_5^2 - 4w_6 > 0$.

5. Applications

In this section, we discuss the motion of submarine (m_3) in the Earth–asteroid–submarine model. The bigger primary is considered as Earth and for the smaller primary, two asteroids namely 216 Kleopatra and 22 Kalliope are considered. The minimum orbit intersection distance (MOID) is used for the distance between the Earth and asteroids. The following physical data has been taken from Lang (1992), Kaur and Aggarwal (2013b), NASA database (https://ssd.jpl.nasa.gov/sbdb.cgi) and Wikipedia (the free encyclopedia).

5.1 *Earth-216 Kleopatra system*

For this system, we have $m_1 = 5.97237 \times 10^{24}$ kg, $a_1 = 6378\,\text{km}$, $a_2 = 6356\,\text{km}$, $\rho_1 = 1027\,\text{kg/m}^3$, $\rho_3 = 1100\,\text{kg/m}^3$, $m_2 = 4.66 \times 10^{18}$ kg, distance between m_1 and $m_2 = 1.09855$ A.U. $= 164340741\,\text{km}$, and $2l = 276\,\text{km}$.

In dimensionless system, $m_1 + m_2 = 1$ unit, that is, 5.97237×10^{24} kg = 1 unit. Thus,

$$\mu = \frac{m_2}{m_1 + m_2} = 7.80259 \times 10^{-7}.$$

The distance between m_1 and m_2 = 1 unit, that is, 164340741 km $= 1$ unit, therefore $l = 8.39719 \times 10^{-7}$, $A = 2.07456 \times 10^{-12}$, $a_1 = 0.0000388096$, $a_2 = 0.0000386757$, $\rho_1 = 7.63237 \times 10^{11}$, $\rho_3 = 8.17489 \times 10^{11}$, $\rho = 0.0663642$, $A_1 = 0.6657446$.

5.2 *Earth-22 Kalliope system*

For this system, we have $m_2 = 8.42 \times 10^{18}$ kg, distance between m_1 and $m_2 = 1.63844$ A.U. $= 245107135\,\text{km}$, $2l = 215\,\text{km}$.

In dimensionless system, $\mu = 1.40982 \times 10^{-6}$, $l = 4.38584 \times 10^{-7}$, $A = 9.32622 \times 10^{-13}$, $a_1 = 0.0000260213$, $a_2 = 0.0000259315$, $\rho_1 = 2.53216 \times 10^{12}$, $\rho_3 = 2.71215 \times 10^{12}$, $\rho = 0.0663643$, $A_1 = 0.6657443$.

For both the presented systems, Earth-216 Kleopatra and Earth-22 Kalliope, it has been observed that L_1 is always an equilibrium point whereas L_2 does not exist, since L_2 dissatisfy the condition of existence, that is, $|x^{(2)}| < a_1$. Also the non-collinear equilibrium points do not exist for both systems, since the existence condition is not fulfilled. In Table 6, the abscissae of the position of the collinear equilibrium points L_1 and L_2 for both systems are calculated for the increasing values of $\epsilon_2 = 0.1, 0.2, 0.3, 0.4, 0.5$. It is observed that for the increasing values of ϵ_2, L_1 drifts away from the centre of m_1 in the left direction. For both the systems, the permissible values of ϵ_1 and ϵ_2 are obtained, that are represented by the light blue color region in Fig. 5 for the stability of the collinear equilibrium point L_1. It is evident that L_1 is stable in both the systems, for all the values of ϵ_1 and ϵ_2 lying in the light blue region.

In Table 7, the stability conditions of L_1 for both systems are calculated for the increasing values of ϵ_1 and ϵ_2 in the range $(-0.9, 0.9)$ with step size 0.2. It is observed that the conditions of stability are satisfied for these combinations of ϵ_1 and ϵ_2, so L_1 is stable.

Table 6. The abscissae of the collinear equilibrium points L_1 and L_2 for the Earth-216 Kleopatra and Earth-22 Kalliope system.

	Earth-216 Kleopatra		Earth-22 Kalliope	
ϵ_2	L_1	L_2	L_1	L_2
0.1	-2.44395×10^{-20}	0.999287	-1.33102×10^{-20}	0.999736
0.2	-4.88789×10^{-20}	0.999287	-2.66204×10^{-20}	0.999736
0.3	-7.33184×10^{-20}	0.999287	-3.99307×10^{-20}	0.999736
0.4	-9.77579×10^{-20}	0.999287	-5.32409×10^{-20}	0.999736
0.5	-1.22197×10^{-19}	0.999287	-6.65511×10^{-20}	0.999736

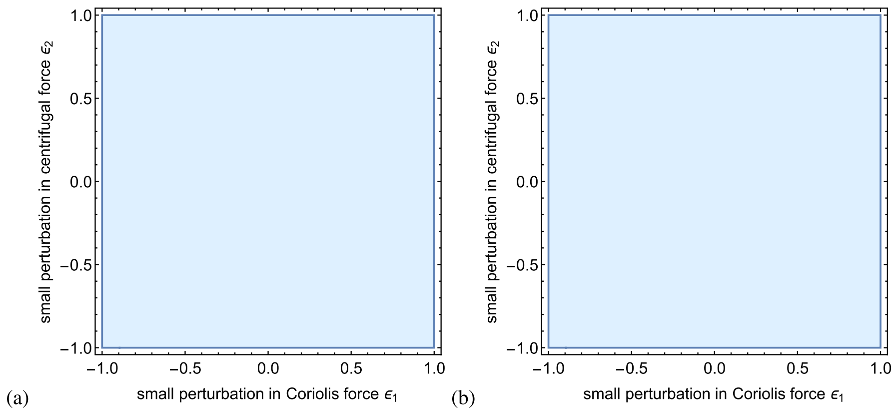

Figure 5. The light blue color region represents the stability conditions (11) (a) for Earth-216 Kleopatra (b) for Earth-22 Kalliope.

Table 7. The stability of the collinear equilibrium point L_1 for the Earth-216 Kleopatra and Earth-22 Kalliope system.

$\epsilon_2 \rightarrow \epsilon_1 \downarrow$	−0.9	−0.7	−0.5	−0.3	−0.1	0.1	0.3	0.5	0.7	0.9
−0.9	stable	stable	stable	stable	stable	stable	stable	stable	stable	stable
−0.7	stable	stable	stable	stable	stable	stable	stable	stable	stable	stable
−0.5	stable	stable	stable	stable	stable	stable	stable	stable	stable	stable
−0.3	stable	stable	stable	stable	stable	stable	stable	stable	stable	stable
−0.1	stable	stable	stable	stable	stable	stable	stable	stable	stable	stable
0.1	stable	stable	stable	stable	stable	stable	stable	stable	stable	stable
0.3	stable	stable	stable	stable	stable	stable	stable	stable	stable	stable
0.5	stable	stable	stable	stable	stable	stable	stable	stable	stable	stable
0.7	stable	stable	stable	stable	stable	stable	stable	stable	stable	stable
0.9	stable	stable	stable	stable	stable	stable	stable	stable	stable	stable

6. Conclusions

In this paper, the impact of small perturbations ϵ_1 and ϵ_2 in the Coriolis and centrifugal forces respectively on the existence, location and stability of the equilibrium points has been studied. It has been observed that these points are also affected by the shape of the primaries that are considered not to be spherical.

This paper focusses on the more general case of Hallan and Mangang (2007). The bigger primary is taken as the hydrostatic equilibrium figure as an oblate spheroid with the oblateness parameter A, that is filled with homogeneous incompressible fluid of density ρ_1. The smaller primary m_2 is considered as a finite straight segment having the length parameter l. The motion of m_3 which is a small solid sphere of density ρ_3 lying inside m_1 is studied under the influence of the small perturbations in the Coriolis and centrifugal forces. In the absence of the parameters ϵ_1, ϵ_2 and l, our results are in accordance with Hallan and Mangang (2007).

We have examined the position of equilibrium points and their stability in the Robe's restricted three-body problem under the combined effects of small perturbations in the Coriolis and centrifugal forces, oblateness and length parameters. The problem possesses two collinear L_1 and L_2, and infinite number of non-collinear equilibrium points. The point L_1 is always an equilibrium point, whereas the point L_2 is an equilibrium point provided $1 - 2\pi\rho_1 A_1 < -\frac{3}{4}\mu$ and $|x^{(2)}| < a_1$.

The position of L_1 is disturbed by the parameters ϵ_2 and A, however L_2 is disturbed by the parameters ϵ_2, A and l. The changes in the positions of L_1 and L_2 with respect to the involved parameters are explained numerically in Tables 1, 2, 3 and graphically in Fig. 1. The non-collinear equilibrium points lie on the circle given by Eq. (5), provided they are inside the bigger primary m_1. The parameters ϵ_2, A and l has a substantial effect on the radius of this circle.

The stability analysis is performed for all the obtained equilibrium points. It is observed that the stability of the equilibrium points is influenced by the parameters ϵ_1 and ϵ_2 due to the small perturbations in the Coriolis and centrifugal forces. Figures 2, 3 and 4 are drawn for a particular set of parameters, to obtain all the possible combinations of ϵ_1 and ϵ_2 for which the equilibrium points L_1 and L_2 are stable.

The present model is more realistic than the ones presented by Hallan and Mangang (2007) and Kumar *et al.* (2019), since we have considered the shape of both the primaries as well as the effect of small perturbations in the Coriolis and centrifugal forces. In Section 5, the motion of any submarine having density ρ_3 greater than the density of m_1 which is ρ_1, has been discussed and some conclusions are made accordingly.

Acknowledgements

The authors are thankful to Centre for Fundamental Research in Space dynamics and Celestial mechanics (CFRSC), New Delhi, India for providing necessary and sufficient research facilities.

References

AbdulRaheem A., Singh J. 2006, Astron. J., 131, 1880
Abouelmagd E. I., Asiri H. M., Sharaf, M. A. 2013, Meccanica, 48, 2479
Aggarwal, R., Kaur, B. 2014, Astrophys. Space Sci., 352, 467
Ansari A. A., Singh J., Alhussain Z. A., Belmabrouk H. 2019, New Astronomy, 73, 101280
Bhatnagar K. B., Hallan P. P. 1978, Celest. Mech. Dyn. Astron., 18, 105
Bhatnagar K. B., Hallan P. P. 1983, Celest. Mech. Dyn. Astron., 30, 97
Deprit A., Deprit-Bartholme A. 1967, Astron. J., 72(2), 173
Giordano C. M., Plastino A. R., Plastino A. 1997, Celest. Mech. Dyn. Astr., 66, 229
Hallan P. P., Mangang K. B. 2007, Planet. Space Sci., 55, 512
Hallan P. P., Mangang K. B. 2008, Advances in Astron., 2008, Article ID 425412, 21 pages
Hallan P. P., Rana N. 2001a, Celest. Mech. Dyn. Astr., 79, 145
Hallan P. P., Rana N. 2001b, Planet. Space Sci., 49, 957
Kaur B., Aggarwal R. 2012, Astrophys. Space Sci., 339, 283
Kaur B., Aggarwal R. 2013a, Acta Astronautica, 89, 31
Kaur B., Aggarwal R. 2013b, Astrophys. Space Sci., 349, 57
Kaur B., Kumar D., Chauhan S. 2020, Astron. Nachr., 341, 32
Kumar D., Kaur B., Chauhan S., Kumar V. 2019, Int. J. Non-Linear Mech., 109, 182
Kushva, B. S. 2008, Astrophys. Space Sci., 315, 231
Lang K. R. 1992, Astrophysical Data: Planets and Stars, Springer, New York
Plastino A. R., Plastino A. 1995, Celes. Mech. Dyn. Astron., 61, 197
Robe H. A. G. 1977, Celes. Mech. Dyn. Astron., 16, 343
Shrivastava A. K., Garain D. 1991, Celes. Mech. Dyn. Astron., 51, 67
Si-hui S. H. U., Ben-kui L. U. 2005, Chinese Astron. and Astrophys., 29, 421
Singh J., Bello N. 2014, Astrophys. Space Sci., 351, 491
Singh J., Haruna S. 2014, Astrophys. Space Sci., 349, 107
Singh J., Mohammed H. L. 2012, Earth Moon Planets, 109, 1
Singh J., Mohammed H. L. 2013, Astrophys. Space Sci., 345, 265
Singh J., Sandah A. U. 2012, Adv. Math. Phys. 18 pages
Subbarao P. V., Sharma R. K. 1975, Astron. & Astrophys., 43, 381
Szebehely V. 1967a, Theory of Orbits, The Restricted Problem of Three Bodies, Academic Press, New York
Szebehely V. 1967b, Astron. J., 72(1), 7
Wintner A. 1941, The Analytical Foundations of Celestial Mechanics. Princeton University Press, Princeton, New Jersey, pp. 372–373